

Studies on palladium-bisphosphine catalyzed alternating copolymerization of CO and ethylene

He-Kuan Luo ^{a,*}, Yuan Kou ^b, Xi-Wen Wang ^c, Da-Gang Li ^c

^a State Key Laboratory for Oxo Synthesis and Selective Oxidation, Lanzhou Institute of Chemical Physics, Chinese Academy of Sciences, Lanzhou 730000, China

^b College of Chemistry and Molecular Engineering, Beijing University, Beijing 100871, China

^c State Key Laboratory for Oxo Synthesis and Selective Oxidation, Lanzhou Institute of Chemical Physics, Chinese Academy of Sciences, Lanzhou 730000, China

Received 15 October 1998; accepted 3 June 1999

Abstract

Palladium(II)-bisphosphine catalyzed copolymerization of CO and ethylene was studied in detail. The results showed that DPPPr/Pd(II) mole ratio, CF₃COOH/Pd(II) mole ratio and solvent greatly influence the catalytic activity. Solvent effects were studied and in detail through end group analysis. With high pressure in situ ¹H-NMR technique, the signals of coordinated ethylene at 4.4 ppm and methylene linked with Pd(II) (Pd—CH₂-) at 0.6 ppm were observed. With high-pressure in situ IR technique three palladium carbonyl absorptions were observed generated at 1638 cm⁻¹, 1616 cm⁻¹ and 1970 cm⁻¹, which may be assigned to three intermediates (3) (5) (6). With the above results, the copolymerization mechanisms were discussed. High-pressure in situ ³¹P-NMR experimental result showed that only mono-chelate ring complex (1) was produced when DPPPr/Pd(II) = 1; only bis-chelate ring complex (2) was produced when DPPPr/Pd(II) = 2; equimolar complex (1) and (2) were produced when DPPPr/Pd(II) = 1.5. Extended X-ray absorption fine structure (EXAFS) was used to calculate the coordination number (CN) and shell radius (*R*, in Å) of complexes (DPPPr)Pd(OCOCF₃)₂ (a), (DPPBu)Pd(OCOCF₃)₂ (b), (DPPEt)Pd(OCOCF₃)₂ (c), (DPPPr)₂Pd(OCOCF₃)₂ (e), and two catalyst solutions of methanol freshly taken before and in the middle of copolymerization (named S1 and S2, respectively). The Pd—P bond length of complexes (a) (b) (c) are 2.25(3) Å, 2.33(3) Å, and 2.38(2) Å, respectively, Pd—O bond length of complexes (a) (b) (c) are 2.07(3) Å, 2.06(2) Å and 2.05(3) Å, respectively. In the order of complexes (a) (b) (c), the catalytic activity increases with Pd—P bond decreasing and Pd—O bond increasing, which may show that the chelate ring is more stable, the anions can go away more easily, and the corresponding catalyst is more efficient. The coordination number of two catalyst solutions S1 and S2 are increased by 1.9 and 0.9 compared with solid complex (a), which may show that 18-electron and five-coordinated pyramidal intermediates were produced and existed in the system besides 16-electron and four-coordinated square planar intermediates. © 2000 Elsevier Science B.V. All rights reserved.

Keywords: Palladium-bisphosphine; CO; Ethylene

* Corresponding author. Beijing Research Institute of Chemical Industry, Beijing 100013, China.

1. Introduction

The copolymerization of CO with ethylene to prepare alternating polyketones has attracted great interest in recent 20 years, especially after the highly efficient palladium(II) catalyst was developed by SHELL [1,2], a large number of researchers were absorbed to study the copolymerization in order to find a cheap and excellent catalyst or modify the highly efficient palladium(II)-bisphosphine catalyst.

About the chain propagation mechanism, Sen first proposed an alternative insertion chain propagation mechanism according to the copolymer analysis [3], and was accepted widely. Drent also proposed a similar but more perfect mechanism also according to the copolymer analysis [4]. But Batistini and Consiglio [5] proposed a new chain propagation mechanism involving cationic Pd—carbene species in order to account for the formation of CO/propylene copolymer with spiroketal repeating units. About this mechanism, Sen [6] and Wong et al. [7] showed strong disagreement with Consiglio. They all believed that polyspiroketal was formed after polyketone was produced under certain conditions, and Sen proved that there existed an interconversion relationship between polyspiroketal and polyketone in certain conditions without metallic palladium.

Chain initiation and termination mechanisms, up to now, were all proposed according to the end-group analysis. Sen first proposed a Pd—H initiation in CHCl_3 solvent. H is coming from trace protic impurity of the system, for example H_2O and CH_3OH . Later, Sen [8] proposed that chain initiation was mainly due to Pd—H and secondarily due to insertion of CO into Pd— OCH_3 bond in CH_3OH solvent. Drent et al. [4] analyzed the end groups of low molecular weight CO/ethylene co-oligomers with GC-MS technique, and found three kinds of general formula polyketones $\text{CH}_3\text{CH}_2(\text{COCH}_2\text{CH}_2)_n\text{COOCH}_3$ (keto-esters), $\text{CH}_3\text{O}(\text{COCH}_2\text{CH}_2)_n\text{COOCH}_3$ (diesters) and $\text{CH}_3\text{CH}_2(\text{COCH}_2\text{CH}_2)_n\text{COCH}_2\text{CH}_3$ (diketones). According to this result, Drent proposed that, chain initiation was firstly and mainly due to insertion of CO into Pd— OCH_3 bond, less Pd—H was produced when chain was terminated as alcoholysis of the palladium—acyl bond, Pd—H can also initiate the copolymerization.

In order to support the alternative chain propagation mechanism, Pd—H initiation and Pd— OCH_3 initiation mechanism, Brumbaugh et al. [9], Dekker et al. [10–12] and Rix et al. [13] have prepared many model complexes, with which olefin insertions into Pd—COR bond and Pd—COOR bond, and CO insertions into Pd—R bond and Pd—OR bond were studied. With complex $(\text{BPy})\text{Pd}(\text{CH}_3)_2$ as model catalyst, and with ^{13}C -NMR technique, Brookhart et al. [25] studied the copolymerization of ^{13}CO with *p*-tertbutyl styrene, observed the carbonyl resonances of the intermediates in the initial several steps of ^{13}CO and *p*-tertbutyl styrene alternative insertions, provided more direct evidence for this copolymerization mechanism.

From the above statements, we can demonstrate that, the real polyketone catalytic systems are highly active, and intermediates are usually too reactive to be isolated or even detected; up to now, mechanisms proposed by researchers are all according to the copolymer analysis [3–8,14], and evidence is not adequate. Therefore, several groups have studied model systems using other ligands (mainly dinitrogen systems) and olefins (styrene, norbornene, norbornadiene) for which intermediates can be detected (by, e.g., NMR or IR) or sometimes isolated. While such model studies provide valuable background information, it is often difficult to translate the results to the real catalytic systems.

Here, we selected real catalytic systems (palladium(II)-bisphosphine catalyst) to study CO/ethylene copolymerization reaction and mechanisms under real reaction conditions. Influence of DPPPPr/Pd(II) mole ratio, CF_3COOH /Pd(II) mole ratio and solvent were studied in details. End groups of polyketones prepared from various solvents were analyzed. High-pressure in situ ^1H -NMR,

^{31}P -NMR and IR techniques were used to study the mechanism under real reaction conditions. Finally, with EXAFS techniques, CN and R (Å) of palladium in catalytic systems were analyzed. These studies provided some more direct and valuable evidence for studying the mechanisms, some results demonstrated from model studies by other groups were translated to the real catalytic systems, and therefore, made the copolymerization mechanisms more perfect.

2. Results and discussion

2.1. Studies on palladium(II)-bisphosphine catalyzed copolymerization of CO with ethylene

2.1.1. Investigations on the effect of DPPPr/Pd(II) mole ratio on CO / ethylene copolymerization

DPPPr/Pd(II) mole ratio has great influence on this copolymerization (see Table 1). Without DPPPr, only palladium(0) black was observed to generate. When DPPPr/Pd(II) = 2.5, only light yellow solution was obtained; under these two conditions copolymerization could not be performed. When DPPPr/Pd(II) is between 0 and 1.5, the catalytic activity was increased rapidly with the increasing of DPPPr/Pd(II) mole ratio. When DPPPr/Pd(II) is between 1.5 and 2.5, the catalytic activity decreased rapidly with the increasing of the DPPPr/Pd(II) mole ratio. This result was rationalized in the following high pressure in situ ^{31}P -NMR studies.

2.1.2. Investigations on the effect of CF_3COOH / Pd(II) mole ratio on CO / ethylene copolymerization

CF_3COOH /Pd(II) mole ratio also has great influence on this copolymerization (see Table 2). Without CF_3COOH , palladium(II)-bisphosphine catalyst has no activity, only palladium(0) black was observed generated, clearly indicating CF_3COOH is an essential component of this catalyst. When CF_3COOH /Pd(II) mole ratio is between 0 and 10, with the increase in CF_3COOH /Pd(II) mole ratio, the catalytic activity increased quickly. When CF_3COOH /Pd(II) mole ratio is above 10, with the increase in CF_3COOH /Pd(II) mole ratio, the catalytic activity increased slowly. The effect of acid or anions may be displayed through its stabilization on cationic palladium(II), and will be further probed in the following EXAFS studies.

2.1.3. Copolymerization in various solvents

2.1.3.1. Copolymerization in various alcoholic solvents. In methanol, the catalyst has the most efficient activity, and with the increase in the carbon number of solvent from methanol to 1-pentanol, the reactivity decreased significantly (see Table 3). One reason may be mass transference rate was lowered with the increase in the degree of solvent viscosity from methanol to 1-pentanol. The other reason may be that the insertion rate of CO into Pd—OR bond was lowered with R group becoming bigger from $-\text{CH}_3$ to $-(\text{CH}_2)_3\text{CH}_3$, which may be the main chain initiation and will be discussed in the following.

Table 1

Effect of DPPPr/Pd(II) mole ratio on CO/ethylene copolymerization

Reaction conditions: Pd(OAc) $_2$ 0.075 mmol, CF_3COOH 0.1 mmol, CH_3OH 40 ml, Pressure 6.0 MPa, CO/ethylene 1:1, 90°C, 1 h.

DPPPr/Pd(II) mole ratio	0	1.25	1.5	2	2.5
Yield (g)	Pd(0)	15.1	18.5	10.0	0
Reaction rate Kg/(gPd h)	0	5.7	7.0	3.8	0

Table 2

Effect of CF₃COOH/Pd(II) mole ratio on CO/ethylene copolymerizationReaction conditions: Pd(OAc)₂ 0.025 mmol, DPPPr 0.0375 mmol, CH₃OH 40 ml, pressure 6.0 MPa, CO:ethylene 1:1, 90°C, 1 h.

CF ₃ COOH/Pd(II) mole ratio	Yield (g)	Reaction rate kg/(gPd h)
0	0	0
1	Trace	~ 0
1.25	1.0	0.38
1.5	2.0	0.75
2	8.5	3.2
3	10.5	3.9
4	12.2	4.6
5	13.2	5.0
10	13.8	5.2
20	14.0	5.3
50	18.5	7.0
62	18.5	7.0

2.1.3.2. *Copolymerization in various nonalcoholic solvents.* The experimental results (see Table 4) showed that, besides methanol and acetone, in propionaldehyde, *N,N*-dimethylformamide, *N,N*-dimethylacetamide, glacial acetic acid, dimethylsulfoxide, the catalyst exhibited moderate efficient activity, especially in glacial acetic acid, the catalytic reaction can proceed without CF₃COOH. But in ethyl ether and acetic ether, the catalyst deactivated completely, palladium(II) was reduced to palladium(0) black observed and mostly deposited on the inner autoclave wall.

Solvent effect will be studied further in the following.

2.2. Mechanistic studies on palladium(II)-bisphosphine catalyst

2.2.1. Chain initiation, termination and solvent effect

Solvent is an important component of the catalytic system, for example, methanol participates the chain initiation and termination; therefore, studies on solvent effect is very useful to probe the catalytic mechanisms, especially for chain initiation and termination mechanisms. Here, end groups of polyketones prepared from different solvents were analyzed with high-resolution NMR technique. The ¹H-NMR data and assignments are listed in Table 5, the ¹³C-NMR data and assignments are listed in Tables 6 and 7, respectively.

From Tables 5–7, we can conclude that the backbone of these polyketones is $-\text{[CH}_2\text{CH}_2\text{CO]}_n-$, in which only very few fragments of two ethylene monomers are linked together. When these spectra are enlarged, the resonances due to end groups are very clear. Because end groups are produced in chain initiations and terminations, chain initiation and termination mechanisms can be induced from the end-group analysis. In this paper, end-group analysis showed that polyketones produced from methanol have two approximately equimolar $-\text{COOCH}_3$ and $-\text{CH}_2\text{CH}_3$. But it is not clear which group is the “head” and which is the “tail” of the polymer; for this reason, high-pressure in situ

Table 3

Copolymerization results in various alcoholic solvents

Reaction conditions: Pd(OAc)₂ 0.025 mmol, DPPPr 0.0375 mmol, CF₃COOH 0.1 ml, solvent 40 ml, pressure 6.0 MPa, CO/ethylene 1:1, 90°C, 1 h.

Solvent	Methanol	Ethanol	1-Propanol	1-Butanol	1-Pentanol
Yield (g)	13.0	10.0	9.1	4.3	1.9
Reaction rate kg/(gPd h)	4.9	3.8	3.4	1.6	0.7

Table 4

Copolymerization results in various nonalcoholic solvents

Reaction conditions: pressure 6.0 MPa, CO/ethylene 1:1, 1 h.

Solvent	Amount of solvent (ml)	Yield (g)	Reaction rate g/(gPd h)	Pd(OAc) ₂ (mmol)	DPPPr (mmol)	CF ₃ COOH (mmol)	Temperature (°C)
Methanol (for comparison)	40	18.5	7000	0.025	0.0375	1.25	90
Acetone	40	6.0	2200	0.025	0.0375	1.25	100
Propionaldehyde	50	9.6	914	0.10	0.15	5.0	95
<i>N,N</i> -Dimethylformamide	50	8.7	828	0.10	0.15	5.0	95
<i>N,N</i> -Dimethylacetamide	50	4.0	381	0.10	0.15	5.0	95
Glacial acetic acid	50	3.5	333	0.10	0.15	5.0	95
Dimethylsulfoxide	50	2.0	210	0.10	0.15	5.0	95
Ethyl ether	50	0	0	0.025	0.0375	1.25	90
Acetic ether	50	0	0	0.025	0.0375	1.25	90

¹H-NMR and IR techniques were used to study this catalytic copolymerization in methanol and 2-ethyl hexanol, respectively (see below). Pd—H signal was not observed in the in situ ¹H-NMR studies near -7 ppm, and in the in situ IR studies near 2050 cm⁻¹. But three IR absorptions due to palladium carbonyl intermediates were trapped successfully, suggested that chain initiation was mainly due to CO insertion into Pd—OR bond, produced end group -COOCH₃ (see Eq. (1)) chain termination was mainly due to the protolysis of palladium-acyl bond, produced end group -CH₂CH₃ (see Eq. (2)). End-group analysis also showed that polyketones prepared from nonalcoholic solvents have predominant end group -CH₂CH₃, and less -CH=CH₂ which was produced by reaction of β-H elimination of palladium-alkyl bond (see Eq. (3)); chain initiation was only from -CH₂CH₃ (see Eq. (4)). Therefore, in nonalcoholic solvent, chain initiation was due to the insertion of ethylene into Pd—H bond (see Eq. (5)). H came from protic impurity of solvent, or trace H₂ in CO comonomer. Chain termination was mainly due to hydrogen activation (see Eq. (6)).

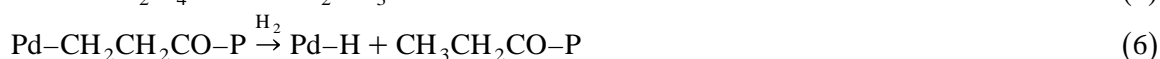
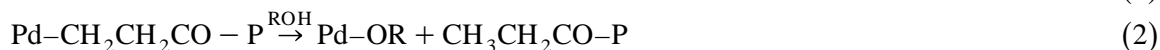


Table 5

¹H-NMR data and assignments of polyketones prepared from various solvents

Solvent	Assignment CH ₃ CH ₂ CO-	CH ₃ CH ₂ CO-	-(CH ₂ CH ₂ CO)-n (main)	-COOCH ₃	-CH ₂ CH ₂ OCH ₃	CH ₂ =CHCO-	CH ₂ =CHCO-
Methanol	1.15(3)	2.68(4)	3.00 (main)	3.84	4.08		
Acetone	1.04(3)	2.55(4)	2.87 (main)			6.07(3)	6.4(2)
Propionaldehyde	1.04(3)	2.56(4)	2.87 (main)				
<i>N,N</i> -Dimethyl- formamide	1.05(3)	2.56(4)	2.88 (main)			6.08(3)	6.4(2)
Glacial acetic acid	1.45(3)	2.97(4)	3.29 (main)				
Dimethyl- sulfoxide	1.65(3)	3.20(4)	3.48 (main)			7.01(3)	6.35(2)

Table 6
 ^{13}C -NMR data of polyketones prepared from various solvents

Solvent	No.											
	1	2	3	4 (main)	5	6	7	8	9	10 (main)	11	12
Methanol	9.53	24.97	30.57	38.77	39.63	43.55	55.60			217.62	219	222.04
Acetone	9.30	24.82		38.82		43.38		108.88	155.06	217.56	219.57	
Propionaldehyde	9.63	25.14		38.92		43.67		109.17	155.38	217.89	219.90	
<i>N,N</i> -Dimethylformamide	9.39	24.89		38.69		43.44		108.93	155.14	217.64	219.66	
Glacial acetic acid	9.01	24.51		38.33		43.11			154.79	217.21	219.20	
Dimethylsulfoxide	10.94	26.5		40.30		44.84			218.68			223.30

The above discussion demonstrated that alcoholic solvent participated in the chain initiation and termination. Although copolymerization can proceed in acetone, propionaldehyde, *N,N*-dimethylformamide, *N,N*-dimethylacetamide, glacial acetic acid and dimethylsulfoxide; in fact, these solvents did not participate the reaction. It seems that non-alcoholic solvent has no influence on this catalytic reaction, only acting as diluent and has no difference. But in fact, it is not (see Table 6). Under the same conditions, but in different non-alcoholic solvent, the catalyst showed significantly different activity, especially in ethyl ether and acetic ether, etc.; the catalyst deactivated completely, palladium(II) was reduced to palladium(0) black, showed clearly that solvent not only act as diluent, but also had suitable stabilization on cationic palladium(II) to assist palladium(II) showing highly efficient catalytic activity. This kind of stabilization may be displayed through coordination of solvent with palladium(II), and will be studied further in the following EXAFS studies.

In conclusion, a solvent has at least two kind of effects. The first is acting as diluent, the second is suitable stabilization on cationic palladium(II), alcoholic solvent has the third one to participate the chain initiation and termination.

2.2.2. High-pressure *in situ* ^{31}P -NMR studies

2.2.2.1. Investigations on DPPPr / Pd(II) mole ratio. When (a) DPPPr/Pd(II) = 0.5, only one signal was observed at 13.26 ppm (1#). When (b) DPPPr/Pd(II) = 1.0, only one signal was observed at

Table 7
 Assignments of ^{13}C -NMR data of polyketones prepared from various solvents

No.	Chemical shift (δ)		Assignments
	Experiment	Calculated	
1	9.53	9.41	$-\text{COCH}_2\text{CH}_3$
2	24.97	24.90	$-\text{COCH}_2\text{CH}_2\text{CH}_2\text{CH}_2\text{CO}-$
3	30.57	30.41	$-\text{CH}_2\text{CH}_2\text{COOCH}_3$
4 (main)	38.77	39.41	$-(\text{CH}_2\text{CH}_2\text{CO})_n-$, $-\text{COCH}_2\text{CH}_3$
5	39.63	39.41	$-\text{CH}_2\text{CH}_2\text{COOCH}_3$
6	43.55	43.32	$-\text{COCH}_2\text{CH}_2\text{CH}_2\text{CH}_2\text{CO}-$
7	55.60	51.4	$-\text{COOCH}_3$
8 (impurity)	108		$-\text{OCOCF}_3$
9 (impurity)	155		$-\text{OCOCF}_3$
10 (main)	217.62		$-(\text{CH}_2\text{CH}_2\text{CO})_n-$
11	219		$-\text{COCH}_2\text{CH}_2\text{CH}_2\text{CH}_2\text{CO}-$
12	222		$-\text{COCH}_2\text{CH}_3$

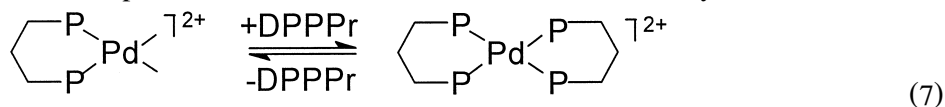
Table 8

In situ ^{31}P -NMR studies on DPPPr/Pd mole ratioConditions: pressure 2.0 MPa, CO/ethylene (1:1), Variation of temperature 40–90°C, 124.5 ppm of 85% H_3PO_4 was used as external standard.

DPPPr/Pd mole ratio	^{31}P -NMR 1#	Chemical 2#	Shift 3#	Activity
0.5	13.26			low
1.0	13.44			high
1.5	14.05	2.27 ~ 1.18		high
2.0		1.93		low
3.0		1.81	- 13.89	none
4.0		1.76	- 14.94	none

13.44 ppm (1#); showing that only mono-chelate ring complex (1) was produced and had highly efficient catalytic activity (see Table 8). When (c) DPPPr/Pd(II) = 1.5, two signals were observed at 14.05 ppm (1#) and 2.27–1.18 ppm (2#) whose integral ratio was 1:2, showing that two equimolar mono-chelate ring complex (1) and bis-chelate ring complex (2) were produced. When (d) DPPPr/Pd(II) = 2.0, only one signal was observed at 1.93 ppm (2#), showing that only bis-chelate ring complex (2) was produced. When (e) DPPPr/Pd(II) = 3.0, two signals were observed at 1.81 ppm (2#) and - 13.89 ppm (3#). When (f) DPPPr/Pd(II) = 4.0, two signals were observed at 1.76 ppm (2#) and - 14.94 ppm (3#). Under conditions of (e) and (f), coordination vacant of palladium(II) were saturated by DPPPr. Besides bis-chelate ring complex (2), free DPPPr existed in the system. Copolymerization result showed that, under these two conditions, the activity deactivated completely.

Table 1 indicates that the catalyst had the most efficient activity when DPPPr/Pd(II) = 1.5. Table 8 indicates that two equimolar mono-chelate ring complex(1) and bis-chelate ring complex (2) were produced. In order to rationalize this result, we proposed a interconversion relationship between these two complexes (see Eq. (7)). During CO/ethylene copolymerization, DPPPr would be decomposed and/or exhausted slowly, then Eq. (7) would shift to the left to ensure the activity of palladium(II). Therefore, although bis-chelate ring complex (2) had no activity, it could increase the total activity and prolong the catalyst life, so palladium(II) exhibited the most efficient activity.



Scheme 1

Scheme 2

In order to probe the existence of a mono-chelate ring complex (1) and bis-chelate ring complex (2), we separately prepared model complexes $(\text{DPPPr})\text{Pd}(\text{OCOCF}_3)_2$ (a) having mono-chelate ring, and $(\text{DPPPr})_2\text{Pd}(\text{OCOCF}_3)_2$ (e) having bis-chelate ring, which were studied further in the following EXAFS studies.

2.2.2.2. In situ ^{31}P -NMR studies under different ambience. No evident chemical shift was observed between under pure ethylene and mixed CO/ethylene (1:1) (see Table 9). Under pure CO, signal 1# of mono-chelate ring complex (1) had significant shift from 14.05 ppm to 5.63 ppm due to coordination of CO with palladium(II), which is coincident with in situ IR result under pure CO. This result suggested that in the competitive coordination of CO and ethylene with palladium, ethylene tends to be easier than CO, or the coordination time of ethylene with palladium was much longer than that of CO.

Table 9

In situ ^{31}P -NMR data under different *ambience*Conditions: $\text{Pd}(\text{OAc})_2$ 0.075 mmol, $\text{DPPPr}/\text{Pd}(\text{II}) = 1.5:1$, CH_3OH 0.8 ml, CF_3COOH 0.2 ml, Pressure 2.0 MPa, 124.5 ppm of 85% H_3PO_4 was used as external standard.

Ambience	Chemical shift	
	1#	2#
Co/ethylene	14.06	2.27 ~ 1.18
Ethylene	13.58	1.92 ~ 1.02
CO	5.63	1.89 ~ 0.98

2.2.3. High-pressure in situ ^1H -NMR studies

2.2.3.1. Studies on coordinated ethylene. First, in situ ^1H -NMR experiment was carried out in CD_3OD , with the temperature rising from 40 to 90°C, free ethylene at 4.9 ppm was observed to decrease rapidly; meanwhile, three signals appeared and increased at 0.6 ppm, 2.9 ppm and 4.4 ppm (see Table 10). With CD_3COCD_3 as solvent, free ethylene at 4.7 ppm was observed to decrease rapidly, and a new signal at 0.5 ppm appeared. In order to assign these new resonances, we designed a series of probe experiments; for example, under pure CO, under pure N_2 , and under $\text{DPPPr}/\text{Pd}(\text{II}) = 2.5$ etc., under these unreactive conditions, no change was observed in the in situ ^1H -NMR spectra at different temperatures.

With CF_3COOD as solvent and under pure ethylene, very strong peak was observed at 1.2 ppm even at ambient temperature. During the temperature raising process, free ethylene at 4.9 ppm decreased rapidly and a new peak at 0.6 ppm appeared. GC-MS analysis indicate $\text{C}_4 =$, $\text{C}_6 =$, $\text{C}_8 =$ were produced, proved that palladium(II)-bisphosphine exhibited high efficient activity for ethylene oligomerization, indicating clearly there is no thermodynamic barrier to ethylene insertion into the Pd—alkyl bonds in this system.

The above result showed that the resonances at 0.6 ppm, 2.9 ppm and 4.4 ppm were only observed under real reaction conditions, did not appear under many unreactive conditions. Compared with the ^1H -NMR spectrum of polyketone, 2.9 ppm was assigned to $-\text{COCH}_2-$ in the backbone, showing

Table 10

New resonances observed in high pressure in situ ^1H -NMRReaction pressure 2.0 MPa, \uparrow Increasing, \downarrow Decreasing.

Solvent	DPPPr/Pd(II) (mol ratio)	Ambience (2.0 MPa)	Temperature (°C)	^1H -NMR data (δ)				Activity
				a	b	c	d	
CD_3OD	1.5:1	$\text{CO}/\text{C}_2\text{H}_4$ 1:1(v:v)	40		2.9		4.9	High
			70	0.6 \uparrow	2.9	4.4 \uparrow	4.9 \downarrow	
CD_3COCD_3	1.5:1	$\text{CO}/\text{C}_2\text{H}_4$ 1:1(v:v)	90	0.5 \uparrow			4.7	High
			40				4.7 \downarrow	
CF_3COOD	1:1	N_2 pure	90					None
			40					
CF_3COOD	1:1	CO pure	90					None
			40				4.9	
CF_3COOD	2.5:1	C_2H_4 pure	90				4.9	None
			40	0.6			4.9	
CF_3COOD	1:1	C_2H_4	90	0.6 \uparrow			4.9 \downarrow	High ^a

^aCatalytic activity of oligomerization of ethylene.

clearly two resonances at 0.6 ppm and 4.4 ppm (1) had close connection with copolymerization, (2) was not due to materials and products, suggesting that these two resonances are due to palladium intermediates. Active center is cationic palladium(II), therefore, intermediates should be cationic palladium(II) complexes, further suggest that these new resonances are due to cationic palladium(II) intermediates.

To resonance at 0.6 ppm, large number of authors [15–18] showed that normal organic compounds did not appear here, but methyl or methylene linked with palladium usually appeared. Therefore, resonance at 0.6 ppm may be due to methyl or methylene linked with palladium contained in intermediates.

To resonance at 4.4 ppm, which appeared at the up-field of free ethylene at 4.9 ppm. Refs. [19,20] showed that coordinated ethylene with palladium appeared near 4.4 ppm in the up-field of free ethylene. Therefore, resonance at 4.4 ppm may be due to coordinated ethylene with palladium. This result showed that before insertion into the Pd—acyl bond to realize chain propagation, ethylene was activated through coordination with palladium.

2.2.3.2. *In situ* $^1\text{H-NMR}$ experiments for Pd–H. Resonance of M–H usually appears in up-field, slightly influenced by other proton resonance, therefore, is easily to be trapped [21–23]. Resonance of Pd–H usually appears near -7 ppm [21,22]. With CD_3OD and CD_3COCD_3 as solvents, Pd–H was not observed, we suspected that Pd–D was produced instead of Pd–H in deuterated solvent. For this reason, we designed and performed a series of *in situ* experiments in CH_3OH instead of CD_3OD . With CH_3OH as solvent and under real reaction conditions, copolymer was observed to produce more and more rapidly with temperature rising from 20 to 90°C , but Pd–H was not observed in up-field. Under unreactive conditions, such as under pure CO, pure N_2 , Pd–H was also not observed. This result indicates that Pd–H concentration was too low to be observed with $^1\text{H-NMR}$ technique. Pd–H was also not observed in *in situ* IR experiments near 2050 cm^{-1} . In conclusion, chain initiation due to Pd–H was slight in alcoholic solvents.

2.2.4. High-pressure *in situ* IR studies

We selected model complex $(\text{DPPPr})\text{Pd}(\text{p-CH}_3\text{PhSO}_3)_2$ as catalyst and 2-ethyl hexanol as solvent, because they have no evident IR absorption between 2200 and 1600 cm^{-1} .

2.2.4.1. *In situ* IR studies under pure CO. At ambient temperature, 4.5 MPa CO was introduced, and immediately, three IR absorptions were observed at 2113 cm^{-1} , 1900 cm^{-1} and 1810 cm^{-1} , and with the temperature rising, 1900 cm^{-1} decreased gradually, 1810 cm^{-1} increased gradually, 2113 cm^{-1} is due to free CO, and 1900 cm^{-1} and 1810 cm^{-1} were difficult to be assigned concretely, but it is no doubt they were due to palladium carbonyl complex, showing clearly CO could coordinate with palladium under pure CO ambience. This result is coincident with *in situ* $^{31}\text{P-NMR}$ under pure CO.

2.2.4.2. *In situ* IR studies under real reaction conditions. In order to control the reaction rate to trap high reactive intermediates, batch experiment technique was used here. First, autoclave was heated to 85°C and pressure of ethylene was controlled at 4.0 MPa. Then, 0.4 MPa CO was introduced, and immediately, *in situ* IR system was recycled and IR spectra were recorded (see Fig. 1). Before CO was introduced, only two absorptions due to free ethylene was observed at 2013 cm^{-1} and 1860 cm^{-1} (see Fig. 1-a). After 0.4 MPa, CO was introduced, four new absorptions immediately appeared at 1690 cm^{-1} , 1670 cm^{-1} , 1638 cm^{-1} and 1616 cm^{-1} (see Fig. 1-b). After reaction for 40 min, a shoulder appeared at 1700 cm^{-1} , at the same time, 1690 cm^{-1} and 1670 cm^{-1} increased, 1638 cm^{-1}

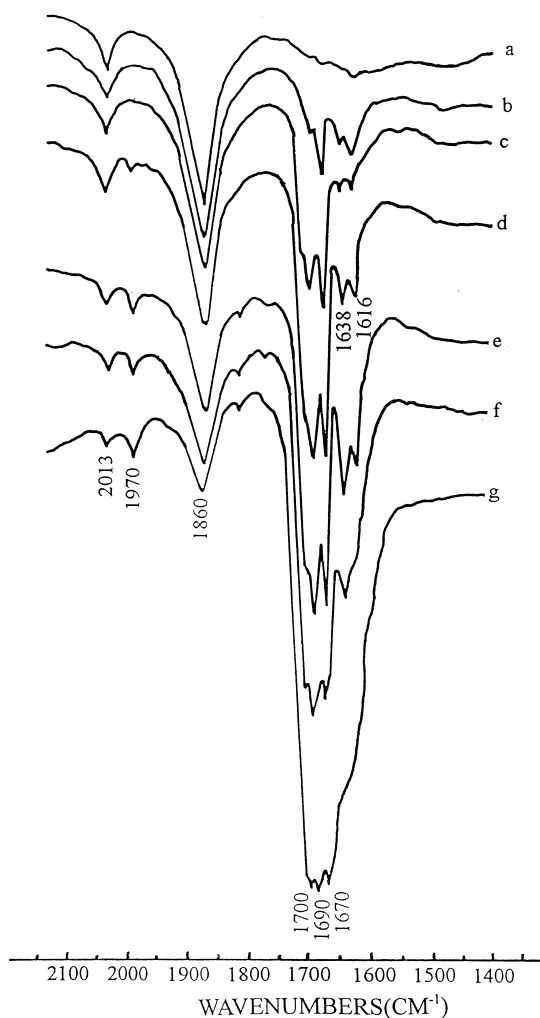


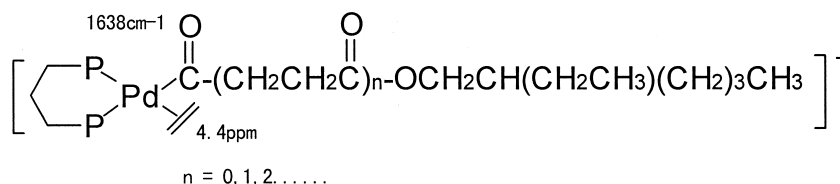
Fig. 1. High-pressure in situ IR spectra under real reaction conditions with $(\text{DPPPr})\text{Pd}(\text{p-CH}_3\text{PhSO}_3)_2$ as catalyst. $(\text{DPPPr})\text{Pd}(\text{p-CH}_3\text{PhSO}_3)_2 = 1$ mmol, $2\text{EH} = 80$ ml. (a) 80°C , 4.0 MPa C_2H_4 . (b) 85°C , introduce 0.4 MPa CO. (c) 85°C , 4.2 MPa, after 40 min. (d) 85°C , 3.8 MPa, after 120 min. (e) 85°C , 3.6 MPa, after 240 min. (f) 85°C , 2.9 MPa, introduce 1.0 MPa CO and after 20 min. (g) 90°C , 2.8 MPa, introduce 1.3 MPa CO and after 30 min.

and 1616 cm^{-1} significantly decreased (see Fig. 1-c). With reaction time being prolonged, these five new absorptions all increased again and became strong, a sixth new absorption appeared at 1970 cm^{-1} (see Fig. 1-d,e). Then 1.0 MPa CO was introduced, 20 min later 1700 cm^{-1} , 1690 cm^{-1} and 1670 cm^{-1} continued increasing, 1638 cm^{-1} decreased significantly, 1616 cm^{-1} disappeared rapidly (see Fig. 1-f). More 1.3 MPa CO was introduced and 30 min later, 1700 cm^{-1} , 1690 cm^{-1} and 1670 cm^{-1} became very strong to form a broad absorption, 1638 cm^{-1} disappeared, 1970 cm^{-1} increased slowly (see Fig. 1-g).

Among these six new absorptions, 1700 cm^{-1} , 1690 cm^{-1} and 1670 cm^{-1} are due to $\nu_{\text{C}=\text{O}}$ absorptions in the polyketones. 1970 cm^{-1} , 1638 cm^{-1} and 1616 cm^{-1} were likely due to palladium carbonyl containing in intermediates, will be assigned in detail in the following.

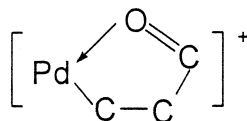
Brumbaugh et al. [9] and Dekker et al. [10–12] have prepared many model complexes, studied the insertions of CO into Pd–R and Pd–OR bonds, and insertions of olefins into Pd–COR and Pd–COOR bonds. This kind of complex has been reported earlier [24].

Refs. [9,10,24] showed that $\nu_{C=O}$ IR absorptions of Pd–COR and Pd–COOR bonds are between 1700 and 1600 cm^{-1} , and significantly influenced by R group, which rule that when R is bigger, the $\nu_{C=O}$ IR absorptions is lower. Therefore, 1638 cm^{-1} were likely due to Pd–COOR in which R is $-(\text{CH}_2\text{CH}_2\text{CO})_n\text{OCH}_2\text{CH}(\text{CH}_2\text{CH}_3)\text{CH}_2\text{CH}_2\text{CH}_2\text{CH}_3$, because here R is big, the $\nu_{C=O}$ IR absorptions is low. Together considering the in situ $^1\text{H-NMR}$ result, we proposed an intermediate (3).

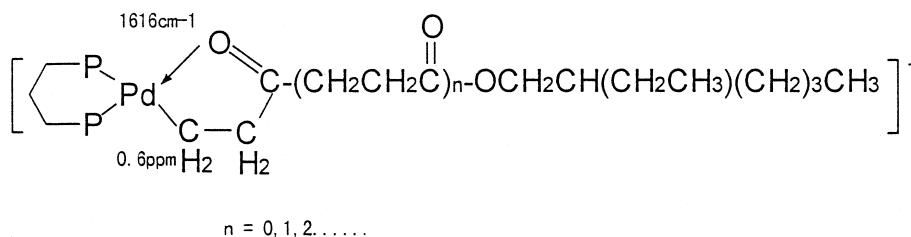


Scheme 3

The literature [9,12] showed that, after the insertions of olefins into Pd–COR and Pd–COOR bonds, $\nu_{C=O}$ IR absorptions all significantly shifted to near 1620 cm^{-1} , because a stable five-membered ring (4) was formed [9]. Therefore, 1616 cm^{-1} was likely due to five-membered ring contained in intermediate (5) produced by intramolecular insertion of coordinated ethylene into Pd–COOR bond in intermediate (3).

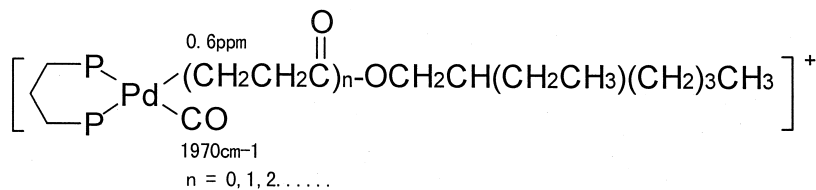


Scheme 4



Scheme 5

1970 cm^{-1} was observed during the copolymerization, was different with that (1900 cm^{-1} and 1810 cm^{-1}) observed under pure CO, therefore, was likely due to a certain intermediate, and Brookhart [25] has trapped the $^{13}\text{C-NMR}$ signal of coordinated CO at low temperature. Here, we suggest that 1970 cm^{-1} was due to intermediate (6).



Scheme 6

2.2.4.3. *About chain initiation and propagation.* The existence of intermediates (3) and (5) showed that chain initiation was firstly and mainly due to CO insertion into Pd–COOR bond, and chain propagation was alternative mechanism. According to these, we proposed a mechanism shown in Scheme 7. With intermediates (3) and (5), the growth and decline rule of 1638 cm^{-1} and 1616 cm^{-1} could be rationalized exactly.

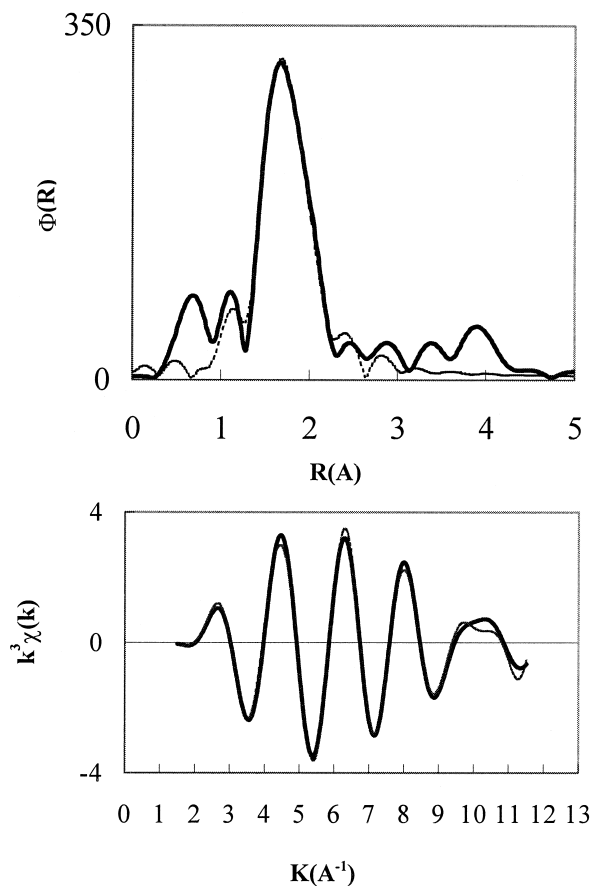
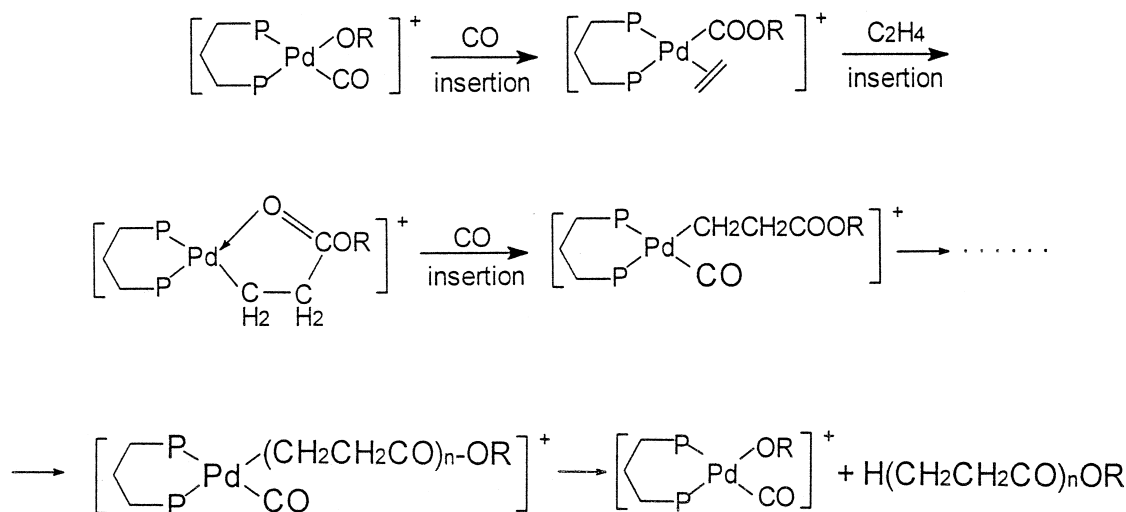


Fig. 2. Best fits (dashed lines) to the Fourier-filtered Pd K-edge EXAFS of (DPPP)PdCl₂ and to the Fourier transform.



In Fig. 1, at the beginning of copolymerization, the pressure of ethylene was much higher than that of CO, 1616 cm^{-1} was stronger than 1638 cm^{-1} (see Fig. 1-b). This is because 1638 cm^{-1} appeared first after CO insertion into Pd–OR bond, and then changed to 1616 cm^{-1} after ethylene insertion into Pd–COOR bond, and the next insertion of CO became slow because the pressure of CO was low. When reaction time was prolonged, most intermediates participated to long chain propagation, therefore, all decreased (see Fig. 1-c). With CO being almost exhausted, the pressure of CO was more low, chain propagation decreased, chain termination increased, and chain initiation was also increased; therefore, 1638 cm^{-1} and 1616 cm^{-1} all grow up gradually, and 1638 cm^{-1} became stronger than 1616 cm^{-1} (see Fig. 1-d,e). When much CO was introduced, the copolymerization rate, especially the insertion rate of CO was significantly increased, 1638 cm^{-1} and 1616 cm^{-1} decreased rapidly. 1616 cm^{-1} disappeared first (see Fig. 1-f), then 1638 cm^{-1} followed (see Fig. 1-g).

2.2.4.4. Comparison of insertion rate of CO with ethylene. Intermediates (3) and (5) were observed together only when pressure of ethylene was much higher than that of CO. After much CO was introduced, intermediate (5) declined immediately. This result indicated clearly that CO insertion was much faster than that of ethylene, according to which we predicted that reaction rate under CO/ethylene < 1 was higher than that of under CO/ethylene = 1. This idea has been proved to be correct in Shell's recent patent [26].

Table 11

Pd K-edge EXAFS-derived CN and R (Å) of standard sample (DPPPr)PdCl₂
 Filtered range (Å), 0.92 ~ 2.63; fitting range in K-space, 1.50 ~ 11.52 (Å⁻¹) with the weight of k^3 .

Shell	EXAFS			Crystal		
	CN	R (Å)	R -factor	CN	R (Å)	R -factor
Pd–P	2.0(2)	2.24(1)	0.12	2	2.244, 2.249	0.027
Pd–Cl	2.4(2)	2.35(1)		2	2.351, 2.358	

Table 12

Pd K-edge EXAFS-derived CN and R (Å) of complexes having general formula (L) Pd(OCOFCF₃)₂

L	Pd–O		Pd–P		R -factor	Filtered range (Å)	Fitting range in K-space with K ³ weight (Å ⁻¹)	Activity order
	CN	R (Å)	CN	(Å)				
DPPPr	2.0(8)	2.07(3)	1.8(7)	2.25(3)	0.14	0.895 ~ 2.557	1.50 ~ 11.52	1
DPPBu	1.4(3)	2.06(2)	1.3(5)	2.33(3)	0.12	0.895 ~ 2.224	1.50 ~ 11.52	2
DPPEt	1.7(6)	2.05(3)	1.2(4)	2.38(3)	0.13	0.869 ~ 2.787	1.50 ~ 11.52	3

2.2.4.5. *Activation of CO.* The existence of intermediate (6) show that CO was activated through coordination with palladium before its insertion. This result was coincident with that of Brookhart [25].

2.2.5. EXAFS studies

Using (DPPPr)PdCl₂(f) as standard sample for calibrating the fitting parameters in this work, CN and R (Å) of central palladium were calculated. Six samples were analyzed. Four solid samples (DPPPr)Pd(OCOFCF₃)₂ (a), (DPPBu)Pd(OCOFCF₃)₂ (b), (DPPEt)Pd(OCOFCF₃)₂ (c), and (DPPPr)₂-

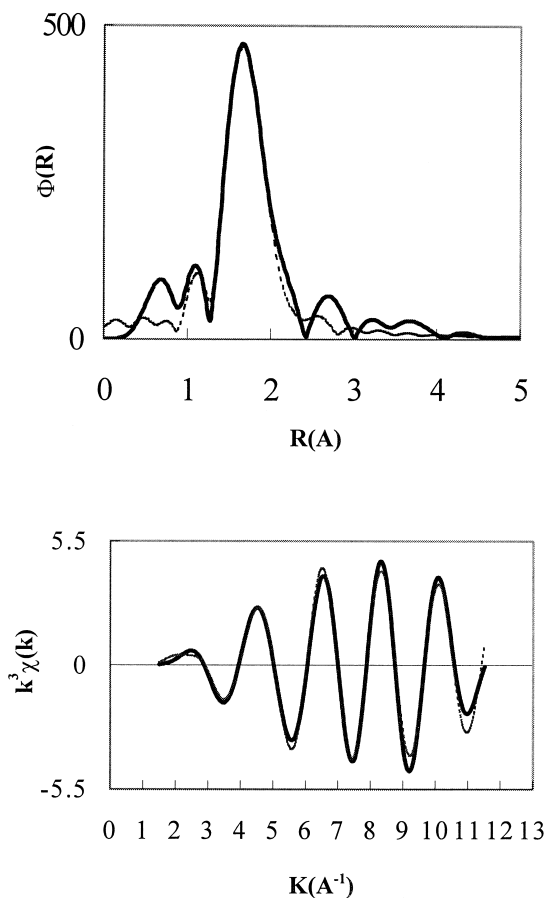


Fig. 3. Best fits (dashed lines) to the Fourier-filtered Pd K-edge EXAFS of (DPPPr)Pd(OCOFCF₃)₂ and to the Fourier transform.

$\text{Pd}(\text{OCOCF}_3)_2$ (e), and two solution samples freshly taken before and in the middle of the copolymerization at $\text{DPPPr}/\text{Pd}(\text{II}) = 1$, were selected.

2.2.5.1. EXAFS analysis of standard sample. Fourier transform and fitting curve in K-space of Pd K-edge EXAFS of $(\text{DPPPr})\text{PdCl}_2$ (f) shown in Fig. 2 showed that experimental curves were well identical with theoretical curves, especially in low K-space. The satisfactory EXAFS-derived parameters and single-crystal data [27] were fixed very closely, especially for R (Å) (see Table 11), provide a reliable technique to study the relationship between catalyst structure and activity.

2.2.5.2. EXAFS studies on ligand effect and anion effect. EXAFS-derived parameters of complexes (a), (b) and (c) are shown in Table 12. Their Fourier transforms and fitting curves in K-space are shown in Figs. 3–5. From Table 12, it can be seen that, with Pd–P bond becoming shorter and with Pd–O bond becoming longer, the catalytic activity was increased significantly, suggesting that chelate ring was more stable and the anion will more easily go away, and the corresponding catalyst had more efficient reactivity. In order to probe the anion effect, the catalytic activity of four complexes having different anions was evaluated and shown in Table 13. CF_3COO^- and $\text{p-CH}_3\text{PhSO}_3^-$ belong to strong acids, have excellent stability to cationic palladium(II), and are weakly coordinated anions,

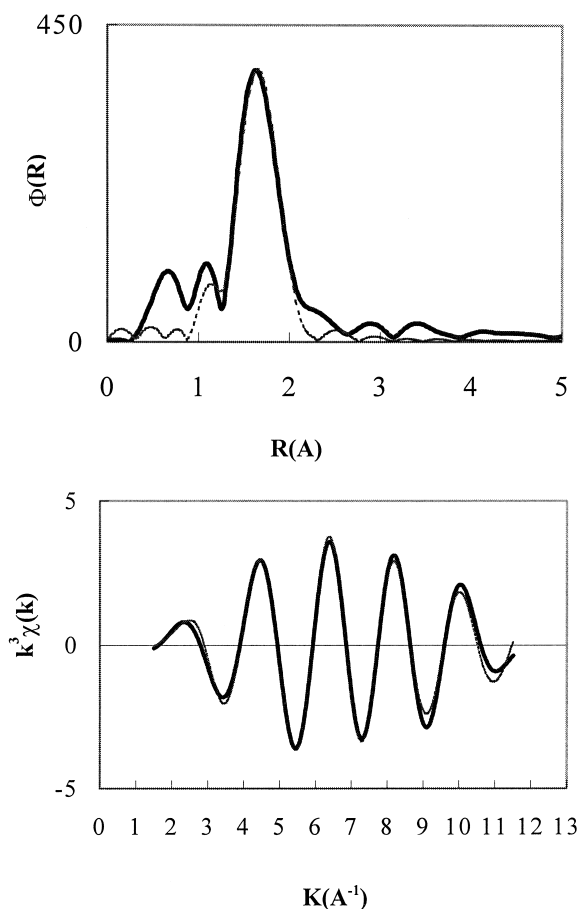


Fig. 4. Best fits (dashed lines) to the Fourier-filtered Pd K-edge EXAFS of $(\text{DPPBu})\text{Pd}(\text{OCOCF}_3)_2$ and to the Fourier transform.

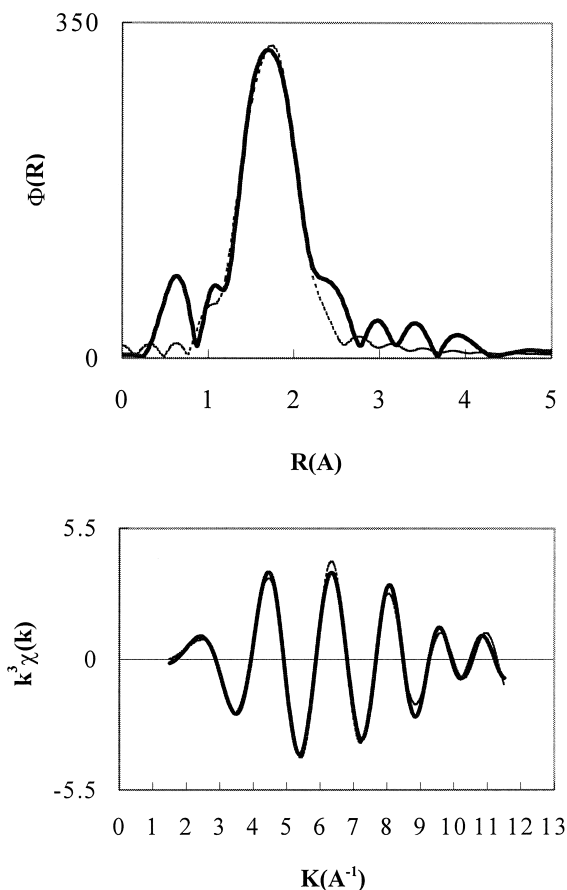


Fig. 5. Best fits (dashed lines) to the Fourier-filtered Pd K-edge EXAFS of $(\text{DPPE})\text{Pd}(\text{OCOCF}_3)_2$ and to the Fourier transform.

easy to go away to leave the coordinate vacant to comonomers; therefore, activity is high. Although Cl^{-1} also belongs to strong acid and has excellent stability to cationic palladium(II), it coordinates with palladium strongly, is very difficult to separate to leave the coordinate vacant to comonomers; therefore, activity is low. $\text{CH}_3\text{COO}^{-1}$ belongs to weak acid, could not stabilize cationic palladium(II) which was reduced to palladium(0) black; therefore, deactivated completely. The above results indicate clearly that a suitable anion first belongs to strong acid, has excellent stability to cationic palladium(II), and easy to split off to leave the coordinate vacant to comonomers.

2.2.5.3. Comparison of mono-chelate ring complex (a) $(\text{DPPPr})\text{Pd}(\text{OCOCF}_3)_2$ with bis-chelate ring complex (e) $(\text{DPPPr})_2\text{Pd}(\text{OCOCF}_3)_2$. EXAFS-derived parameters of complexes (a) and (e) are listed in Table 14. Their Fourier transforms and fitting curves in K-space were respectively shown in Figs. 3 and 6. From Table 14, it can be seen that the Pd–P bond and Pd–O bond of complex (a) were much shorter than that of complex (e), indicating clearly that complex (a) was more stable than complex (e), providing direct evidence for their interconversion relationship drawn from in situ ^{31}P -NMR.

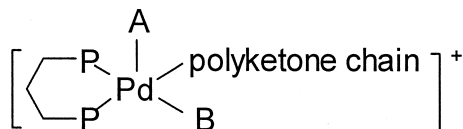
2.2.5.4. EXAFS studies on solution samples freshly taken before and in the middle of the copolymerization at $\text{DPPPr} / \text{Pd(II)} = 1$. EXAFS-derived parameters of complex (a) and two solution samples are listed in Table 15; their Fourier transforms and fitting curves in K-space are shown in Figs. 3, 7

Table 13

Evaluation results of complexes having general formula (DPPPr)Pd(A)₂Conditions: complex 0.025 mmol, CH₃OH 40 ml, CO/ethylene (1:1) 6.0 MPa, 90°C, 1 h.

A ⁻	Yield (g)	Reaction rate kg/(gPd h)
CF ₃ COO ⁻	10.0	3.76
p-CH ₃ PhSO ₃ ⁻	7.6	2.86
Cl ⁻	0.95	0.357
CH ₃ COO ⁻	Pd(0)	0

and 8. It can be found that coordination number of sample S1 (CN = 3.0 + 2.7 = 5.7) and sample S2 (CN = 2.6 + 2.1 = 4.7) significantly increased by 1.9 and 0.9, respectively, compared with solid sample (a) which is four-coordinated. Therefore, d⁸, 18-electron and five coordinated pyramidal species (see Scheme 8) likely existed in the system besides d⁸, 16-electron and four-coordinated square planar species, showing that (1) solvent could coordinate with palladium and therefore, had significant influence on the activity, (2) five-coordinated intermediates may have existed and acted as important actors in the catalytic copolymerization.



Scheme 8

A and B are ethylene or CO or solvent molecular

3. Experimental

3.1. General considerations

Carbon monoxide is the product of Lanzhou Chemical Physics Institute of Academia Sinica. Ethylene is the product of polymer grade of 303 plant of Lanzhou Petroleum Chemical. Pd(OAc)₂ was prepared by myself. Ethyl ether was dried and purified with standard method and freshly distilled before use under N₂. Other solvents and reagents were of commercial grade.

Table 14

Comparison of Pd K-edge EXAFS-derived parameters of mono-chelate ring complex (a) (DPPPr)Pd(OCOCF₃)₂ with bis-chelate ring complex (e) (DPPPr)₂Pd(OCOCF₃)₂

Complex	Pd–O		Pd–P		R-factor	Filtered range (Å)	Fitting range in K-space with K ³ weight (Å ⁻¹)
	CN	R (Å)	CN	R (Å)			
(a)	2.0(8)	2.07(3)	1.8(7)	2.25(3)	0.14	0.895 ~ 2.557	1.50 ~ 11.52
(e)	2.0(5)	2.33(2)	4.9(5)	2.38(1)	0.08	0.920 ~ 2.889	1.50 ~ 11.52

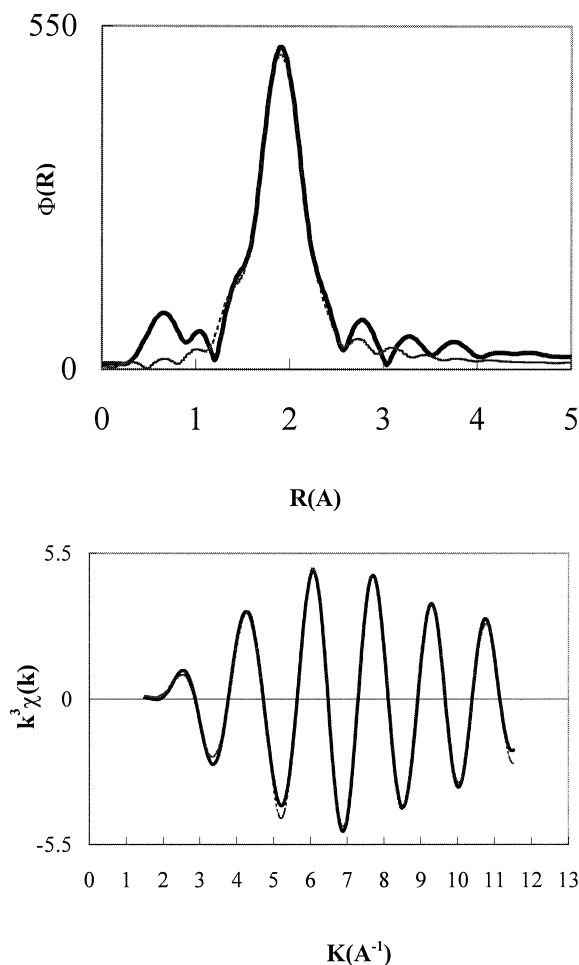


Fig. 6. Best fits (dashed lines) to the Fourier-filtered Pd K-edge EXAFS of $(\text{DPPPr})_2\text{Pd}(\text{OCOCF}_3)_2$ and to the Fourier transform.

In situ NMR spectra and normal NMR spectra of complexes were recorded on a varian FT-80A spectrometer. NMR spectra of polyketones were recorded on a Bruker AM400 spectrometer. In situ IR and normal IR spectra were recorded on a Spexord 75 IR spectrometer.

3.2. General procedure for CO / ethylene copolymerization

Copolymerization was carried out in a 200 ml stainless steel autoclave. First, catalyst precursor or components were added to the reactor; immediately, the reactor was sealed and was purged with

Table 15
Comparison of solid sample (a) with solution samples of EXAFS-derived CN and R (Å)

Code name	Pd–O		Pd–P		R -factor	Filtered range (Å)	Fitting range in K-space with K^3 weight (Å ⁻¹)
	CN	R (Å)	CN	(Å)			
(a)	2.0(8)	2.07(3)	1.8(7)	2.25(3)	0.14	0.895 ~ 2.557	1.50 ~ 11.52
S1	3.0(3)	2.08(2)	2.7(12)	2.19(4)	0.15	0.895 ~ 2.429	1.50 ~ 11.52
S2	2.6(6)	2.08(2)	2.1(9)	2.22(4)	0.14	0.895 ~ 2.506	1.50 ~ 11.52

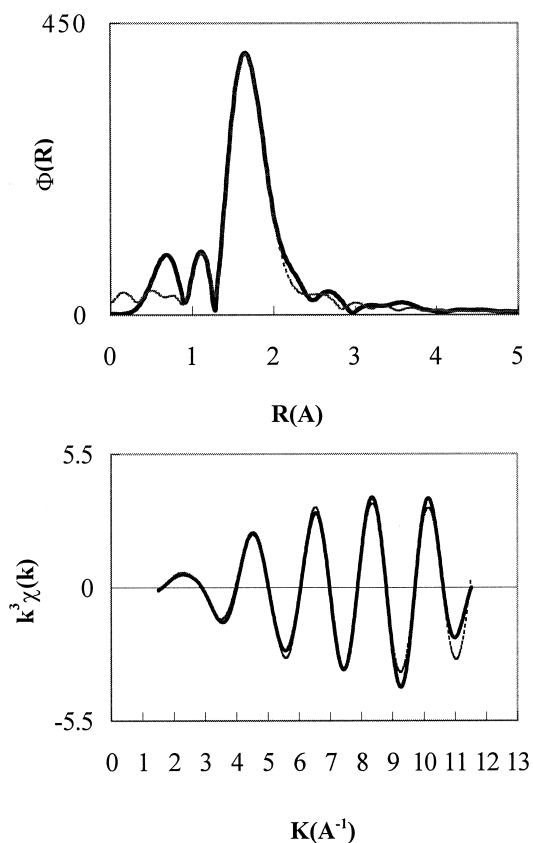


Fig. 7. Best fits (dashed lines) to the Fourier-filtered Pd K-edge EXAFS of S1 and to the Fourier transform.

ethylene at least three times, then the solvent was introduced and ethylene was charged to chosen pressure. After the reactor was heated to the chosen temperature in 30 min, equimolar CO was introduced and total pressure was controlled at about 6.0 MPa during the copolymerization by introducing equimolar CO and ethylene. After reaction for 1 h, the autoclave was rapidly cooled, and the unreacted gases were vented. The product slurry was filtered off, washed with fresh methanol, and dried in the air to give snow-white powder. The average catalytic activity was calculated from copolymer weight as unite of g polyketone/(gPd h).

3.3. *In situ* NMR experiments

High-pressure *in situ* NMR technique developed by Da-Gang Li et al. [28] was used. The *in situ* NMR tube ($\phi = 10$ mm), in fact, is a transparent micro-reactor of homogeneous reaction. Therefore, NMR determination can be carried out under real reaction conditions, and the phenomenon can be observed clearly during the copolymerization.

3.3.1. Representative procedure for *in situ* NMR experiments

Catalyst components and solvent were taken exactly and added into the *in situ* NMR tube; immediately, the tube was sealed and was purged with ethylene at least three times, and was charged with 2.0 MPa equimolar CO and ethylene. NMR spectra were recorded with the temperature rising from 20°C to 90°C.

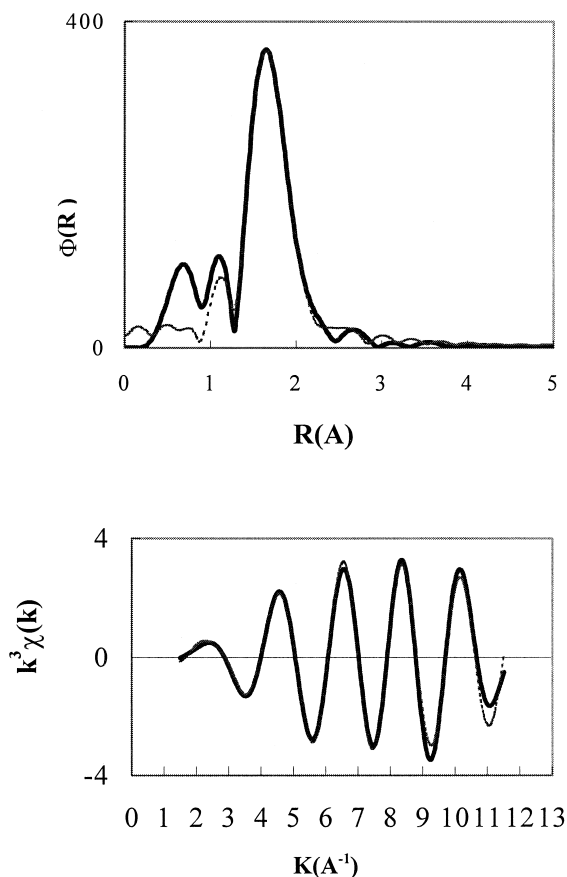


Fig. 8. Best fits (dashed lines) to the Fourier-filtered Pd K-edge EXAFS of S2 and to the Fourier transform.

3.4. In situ IR experiments

High-pressure in situ IR system developed by Wu et al. [29] was used here. 200 ml stainless steel autoclave was used to perform the copolymerization. Two CaF_2 crystals were used as the high-pressure IR cell. Sample space were controlled about 0.2 mm thick. Normal KBr IR cell was used to deduct solvent absorption in sample. 2-Ethyl hexanol was used as solvent.

1.0 mmol $(\text{DPPPr})\text{Pd}(\text{p-CH}_3\text{PhSO}_3)_2$ was added into 200 ml reactor, immediately the reactor was sealed and was purged with ethylene at least three times. Then ethylene was introduced and reactor was heated to 85°C and ethylene pressure was controlled 4.0 MPa, and then 0.4 MPa, 1.0 MPa and 1.3 MPa CO was introduced separately in periodic order; at the same time IR spectra were recorded.

3.5. EXAFS

X-ray absorption spectra were obtained in fluorescence mode (solid samples) and transmission mode (liquid samples) using the BL-7C facility at the Photon Factory (Tsukuba, Japan). A Si(111) double-crystal (Sagittal focusing) monochromator with a position beam energy of 2.5 GeV and an average stored current of 250 mA was employed.

The data were processed on a COMPAQ 486 microcomputer with the Program Library for EXAFS Data Analysis written by the Institute of Physics, Chinese Academy of Sciences [30]. The Fourier transform containing the peaks of interest was filtered into K-space by a Hanning window function.

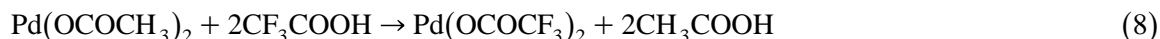
A least-squares current-fitting procedure was then performed to calculate the structural parameters per each shell using theoretically calculated components determined by program FEFF 3.25 developed by Rehr et al. [31] and Mustre et al. [32]. The structural parameters (CN and R in Å) with which the FEFF was started were corrected repeatedly until they were identical to the fitting parameters. The reduction factor used, S_o^2 was 1.1. The best fit of fitting curves was first chosen by an R factor, then was transformed into R-space weighted by K^o with the same range to give a fit of the Fourier transform. The parameter error estimates were calculated by the recommended method [33].

3.6. Preparation of complexes

3.6.1. Preparation of (DPPPr)Pd(OCOCF₃)₂ (a)

The following operations were under Ar ambience. To a 100 ml glass bottle, Pd(OAc)₂ 224.6 mg (1.0 mmol), 25 ml dry ethyl ether and 0.2 ml CF₃COOH was added and stirred for 10 min. Exchange of anions was performed (see Eq. (8)), and orange solution was obtained, to which 412.2 mg (1.0 mmol)/25 ml dry ethyl ether solution was added dropwise with stirring (see Eq. (9)) pale yellow powder was precipitated. The suspension was stirred for 1 h. Pale yellow powder was filtered, washed with dry ethyl ether and dried in vacuum. 592.4 mg (DPPPr)Pd(OCOCF₃)₂ was obtained, Yield 80%.

³¹P-NMR: δ 13.44 (CD₃OD)



Similar procedure was used for the preparation of other six complexes as follows: (DPPBu)Pd(OCOCF₃)₂ (b), Yield 70.9%, ³¹P-NMR: δ 29.24 (CDCl₃); (DPPEt)Pd(OCOCF₃)₂ (c), Yield 78.7%, ³¹P-NMR: δ 61.09 (CDCl₃); (DPPPr)Pd(p-CH₃PhSO₃)₂ (d), Yield 85%, ³¹P-NMR: δ 25.58 (CDCl₃); (DPPPr)₂Pd(OCOCF₃)₂ (e), Yield 55.6%, ³¹P-NMR: δ -2.46 (CDCl₃); (DPPPr)PdCl₂ (f), Yield 76%, ³¹P-NMR: δ 10.72 (DMSO-d₆); (DPPPr)Pd(OCOCH₃)₂ (g), Yield 81.1%, ³¹P-NMR: δ -9.4 (CDCl₃)

4. Conclusions

Palladium(II)-bisphosphine catalyzed copolymerization of CO and ethylene was studied in detail. The results showed that DPPPr/Pd(II) mole ratio, CF₃COOH/Pd(II) mole ratio and solvent all greatly influence the catalytic activity. Solvent effect studies showed that suitable solvent not only act as diluent, but also had perfect stability on cationic palladium(II). Furthermore, alcoholic solvent participated the chain initiation and termination. End-group analysis, in situ NMR, in situ IR and EXAFS studies provided many direct and valuable evidences for mechanistic studies, with which many questions were made more clearly, and some new viewpoints were first proposed and explained, as follows.

(1) In alcoholic solvents, chain initiation was firstly and mainly due to CO insertion into Pd-OR bond; in nonalcoholic solvents, chain initiation was mainly due to ethylene into Pd-H bond, deduced from end group analysis, in situ ¹H-NMR and in situ IR studies.

(2) When DPPP_r/Pd(II) mole ratio was between 1 and 2, mono-chelate ring complex(1) had interconversion relationship with bis-chelate ring complex(2) in the catalytic system, deduced from in situ ³¹P-NMR studies and EXAFS analysis.

(3) CO and ethylene were activated through coordination with cationic palladium(II) before their insertions, deduced from in situ ¹H-NMR and in situ IR studies.

(4) In competitive coordination to vacant sites of palladium(II) species, ethylene exhibited significant superiority compared with CO, deduced from in situ ³¹P-NMR studies.

(5) Insertion of CO was much faster than that of ethylene, deduced from in situ IR studies.

(6) Stable five-member ring intermediate was proved to be produced during copolymerization, deduced from in situ IR studies.

(7) Solvent molecular was in competitive coordination with comonomer to vacant site of palladium(II); therefore, significantly influence the catalytic activity, deduced from solvent effect studies and EXAFS analysis.

(8) For complexes (a), (b) and (c), the chelate ring was more stable, the corresponding complex was more efficient, deduced from EXAFS analysis.

(9) Suitable anions are of strong acid, had excellent stability on cationic palladium(II), and easy to go away to leave coordination vacant to comonomers, deduced from solvent effect studies and EXAFS analysis.

(10) 18-electron, five coordinated pyramidal intermediates was probably produced and existed in the system, beside 16-electron, four-coordinated square planar intermediates, deduced from EXAFS analysis.

Acknowledgements

We are grateful to the Photon Factory for the use of BL-7C Facilities. We thank Dr. T. Tanaka and Professor M. Nomura for experimental assistance. We also thank Kong Suling of Lanzhou University and Zhang Hui of Beijing University for their friendly help.

References

- [1] E. Drent, EP0181014, 1985.
- [2] E. Drent, US4818810, 1989.
- [3] A. Sen, T.W. Lai, *J. Am. Chem. Soc.* 104 (1982) 3520.
- [4] E. Drent, J.A.M. Van Broekhoven, M.J. Doyle, *J. Organomet. Chem.* 417 (1991) 235.
- [5] A. Batistini, G. Consiglio, *Organometallics* 11 (1992) 1766.
- [6] A. Sen, *Acc. Chem. Res.* 26 (1993) 303.
- [7] P.K. Wong, J.A. Van Doorn, E. Drent et al., *Ind. Eng. Chem. Res.* 32 (1993) 986.
- [8] Z. Jiang, G.M. Dahlen, K. Houseknecht, A. Sen, *Macromolecules* 25 (1992) 2999.
- [9] J.S. Brumbaugh, R.R. Whittle, M. Parvez, A. Sen, *Organometallics* 9 (1990) 1735.
- [10] G.P.C.M. Dekker, C.J. Elsevier, K. Vrieze, *Organometallics* 11 (1992) 1598.
- [11] G.P.C.M. Dekker, A. Buijs, C.J. Elsevier et al., *Organometallics* 11 (1992) 1937.
- [12] G.P.C.M. Dekker, C.J. Elsevier, K. Vrieze et al., *J. Organomet. Chem.* 430 (1992) 357.
- [13] F.C. Rix, M. Brookhart, P.S. White, *J. Am. Chem. Soc.* 118 (4746) (1996) .
- [14] F.Y. Xu, A.X. Zhao, J.C. Chien, *Makromol. Chem.* 194 (1993) 2579.
- [15] W. de Graaf, J. Boersma, G. Van Koten, *Organometallics* 9 (1990) 1479.
- [16] A. Gille, J.K. Stille, *J. Am. Chem. Soc.* 102 (1980) 4933.
- [17] F. Ozowa, T. Ito, A. Yamamoto, *J. Am. Chem. Soc.* 102 (1980) 6457.
- [18] M. Rudler-Chauvin, H. Rudler, *J. Organomet. Chem.* 134 (1977) 115.

- [19] F. Ojama, T. Ito, Y. Nakama, A. Yamamoto, J. Organomet. Chem. 168 (1979) 375.
- [20] H. Kurosawa, T. Majima, N. Asada, J. Am. Chem. Soc. 102 (1980) 6996.
- [21] V.N. Zudin, V.D. Chinakov, V.M. Nekipelov et al., J. Organomet. Chem. 289 (425) (1985) .
- [22] V.N. Zudin, V.D. Chinakov, V.M. Nekipelov et al., J. Mol. Catal. 52 (1989) 27.
- [23] D.-G. Li, C.-G. Xia, Y.-W. Sun, WuLi HuaXue XueBao 12 (1) (1996) 71.
- [24] S. Otsuta, A. Nakamura, T. Yoshida, M. Naruto, K. Actaka, J. Am. Chem. Soc. 95 (3180) (1973) .
- [25] M. Brookhart, F.C. Rix, J.M. Desimone, J. Am. Chem. Soc. 114 (1992) 5894.
- [26] J.A. Bakkum, A.M. Bradfor, A. Buys et al., WO 95/29946, 1995.
- [27] W.L. Steffen, G.J. Palenik, Inorg. Chem. 15 (10) (1976) 2432.
- [28] D.-G. Li, C.-G. Xia, Y.-W. Sun, Chinese Patent NO. 28312, 1989.
- [29] G.-S. Wu, D.-G. Li, S.-Q. Xue, YouJi HuaXue 1 (1983) 29.
- [30] Y. Kou, H.L. Wang, M. Te, T. Tanaka, M. Normura, J. Catal. 141 (1993) 660.
- [31] J.J. Rehr, J. Mustre de Leon, S.I. Zabinsky, R.C. Albers, J. Am. Chem. Soc. 113 (1991) 5135.
- [32] J. Mustre, J.J. Rehr, S.I. Zabinsky, R.C. Albers, Phys. Rev. B 44 (1991) 4146.
- [33] F.W. Lytle, D.E. Sayers, E.A. Stern, Physica B 158 (1989) 701.